Supporting Information

Patel et al. 10.1073/pnas.1013715108

SI Materials and Methods

Antibodies and Reagents. Antibodies used in this studied were purchased or provided as follows: Artemis rabbit polyclonal (Orbigen), ATM mouse monoclonal 2C1 (Santa Cruz), BRCA1 rabbit polyclonal and Ku80 rabbit polyclonal (Cell Signaling Technologies), BRCA2 mouse monoclonal 2B (Calbiochem), DNA-dependent protein kinase catalytic subunit (DNA-PKcs) mouse monoclonal 42-pcs (Biosource International), poly(ADP-ribose) polymer rabbit polyclonal 96–10 and poly(ADP-ribose) polymerase 1 (PARP1) mouse monoclonal C2-10 (G. Poirier, Université Laval, Quebec, CA), phospho-Ser^{2056} DNA-PKcs rabbit polyclonal (Abcam), phospho-Thr^{2609} DNA-PKcs rabbit polyclonal (Z. Lou, Mayo Clinic), histone H1 mouse monoclonal (J. Sorace, Veterans Affairs Medical Center, Baltimore, MD), phospho-Ser^{139} histone H2AX mouse monoclonal JBW301 (Millipore), Hsp90β mouse monoclonal (D. Toft, Mayo Clinic), and XRCC1 rabbit polyclonal (Bethyl Laboratories). AZD2281 was obtained from ChemieTek.

Cell Culture. PEO1 and PEO4 cells (1), a kind gift of F. Couch (Mayo Clinic), were cultured in DMEM containing 10% (vol/vol) heat-inactivated FCS, 100 μM nonessential amino acids, and 10 μg/mL insulin (medium A). BRCA1-deficient HCC1937 and reconstituted HCC1937/BRCA1 cells (2) were a kind gift from J. Chen (M. D. Anderson Cancer Center, Houston, TX), and were cultured in RPMI 1640 medium containing 10% (vol/vol) FCS (medium B). M059J and M059J+DNA-PKcs cell lines (a kind gift of L. Karnitz, Mayo Clinic) were grown in DMEM/F-12 (1:1) medium supplemented with 15% (vol/vol) FCS (medium C). GM16666 and GM16667 cell lines were purchased from the Coriell Institute (Camden, NJ) and cultured in DMEM supplemented with 10% (vol/vol) FCS (medium D) and 100 μg/mL hygromycin. CAPAN1 cells were cultured in RPMI 1640 medium containing 15% (vol/vol) FCS (medium E). All media contained 100 units/mL penicillin G, 100 μg/mL streptomycin, and 2 mM glutamine.

siRNA/shRNA Transfection. All siRNA oligonucleotides were purchased from Ambion. Sequences, with references, are provided in the next section. PEO1 and PEO4 cells were transfected with 150 pmol of siRNA by using the HiPerFect lipid transfection reagent (Qiagen). On day 1, $8–10 \times 10^5$ cells were plated onto 6-well dishes in 2.4 mL of antibiotic-free medium and incubated for 24 h in siRNA–lipid complex (150 pmol + 12 μL of HiPerFect in 120 μL of sterile RPMI medium). On day 2, cells were washed with sterile RPMI medium, and the transfection procedure was repeated. On day 3, cells were trypsinized, replated onto 100-mm tissue culture dishes, and grown in medium A. On day 4, cells were harvested for immunoblotting, immunofluorescence, or clonogenic assays as described below. For short hairpin–mediated knockdown in M059J and M059J+DNA-PKcs cells, $5–10 \times 10^6$ cells were electroporated at 240 mV for 10 ms with a square-wave electroporator (BTX Systems). Mission shRNA constructs (Sigma-Aldrich) targeting BRCA1 are listed below. Clonogenic assays and protein harvest were performed 48 h after electroporation.

siRNA Sequences. siRNA sequences used in this study along with references were as follows: Artemis-1, 5′-CUGAAGAGAGCUAGAACAGAA-3′ (3); Artemis-2, 5′-UUA GGAGUCCAGGUUCAUGAA-3′ (3); Ku80-1, 5′-GCGAGUAACCAGCUCAUAAUU-3′ (4); Ku80-2, 5′-AAGAGCUAAUCCUCAAGUCUU-3′ (5); luciferase control, 5′-CUUACGCUGAGUACUUCGAUU-3′; PARP1-1, 5′-AAGCCUCCGCUCCUGAAC AAU-3′ (6); PARP1-2, 5′-AAGAUAGAGCGUGAAGGCGAA-3′ (6); XRCC1-1, 5′-AGGGAAGAGGAAGUUGGAUUU-3′ (7); and XRCC1-2, 5′-CUCGACUCACUGUGCA GAAUU-3′ (8). Mission shRNA sequences (Sigma-Aldrich) were as follows: shBRCA1 #1 (Hx72), 5′-CCGGCCCACCTAATTGTACTGAATTCTCGAGAATTCAGTACAAT TAGGTGGGTTTTTG-3′; and shBRCA1 #2 (Hx75), 5′-CCGGCCCTAAGTTTACTTCTCTAAACTCGAGTTTAGAGAAGTAAACTTAGGGTTTTTG-3′.

Clonogenic Assays. Colony-formation assays were performed on siRNA-transfected PEO1 and PEO4 cells 48 h after the second transfection. Cells were trypsinized and plated at 750 cells per plate in triplicate 60-mm dishes containing medium A, allowed to grow for 10–14 d, and stained with Coomassie Brilliant Blue. Colonies containing ≥50 cells were scored manually. To assess methyl methanesulfonate (MMS) sensitivity, PEO1 or PEO4 cells were incubated for 48 h after the second siRNA treatment, plated onto 60-mm dishes, allowed to adhere for 4 h, exposed to the indicated concentration of MMS (Sigma-Aldrich) for 1 h, washed with sterile RPMI 1640 medium, and allowed to grow into colonies in medium A. For drug treatment, cells (without siRNA) were allowed to adhere for 4–6 h, then treated with the indicated concentrations of ABT-888 and/or AZ12594248 for 72 h. After drug treatment, cells were washed with drug-free RPMI 1640 medium, cultured for 10–14 d in medium A, and stained. For HCC1937 and HCC1937/BRCA1 cells, a similar procedure was used with several changes: 1,000 cells were plated in medium B, and treatment was continuous for 16–20 d. M059J and M059J+DNA-PKcs were plated at 1,000 cells per plate in medium C and treated for 48 h. GM16666 and 16667 were plated at 1,000 cells per plate in medium D and treated for 48 h.

Immunoblotting. Cells were washed twice with calcium- and magnesium-free Dulbecco's PBS and solubilized in 6 M guanidine hydrochloride containing 250 mM Tris·HCl (pH 8.5 at 20 °C), 10 mM EDTA, 1% (vol/vol) 2-mercaptoethanol, and 1 mM freshly added phenylmethylsulfonyl fluoride. After preparation for electrophoresis as described previously (9), aliquots containing 50 μg of protein (determined by the bicinchoninic acid method; ref. 10) were separated on SDS/polyacrylamide gels containing 8% (wt/vol) acrylamide, electrophoretically transferred to nitrocellulose, and probed with immunological reagents as described (11). Finally, 6% polyacrylamide gels were used to resolve the DNA-dependent protein kinase (DNA-PK), and 4–20% gradient polyacrylamide gels were used to resolve histones.

Immunofluorescence and Confocal Microscopy. Immunofluorescence studies were performed as described by Segovis et al. (12) with several modifications. Cells grown on nitric acid–etched coverslips were treated as described, then fixed in 2% (wt/vol) paraformaldehyde in PBS for 10 min at room temperature, washed with PBS, and permeabilized with 0.25% (vol/vol) Triton X-100 in PBS for 5 min. Coverslips were then incubated in blocking buffer consisting of PBS, 1% (vol/vol) glycerol, 0.1% (wt/vol) gelatin from cold-water fish, 5% (vol/vol) normal goat serum, 0.1% (wt/vol) BSA, and 0.4% (wt/vol) sodium azide for 1 h at room temperature. Coverslips were incubated overnight at 4 °C in primary antibody (1:500 dilution for phospho-Ser^{139} H2AX, 1:250 for phospho-Thr^{2609} DNA-PKcs, or 1:250 for phospho-Ser^{2056} DNA-PKcs). Coverslips were then washed three times with PBS and incubated for 1 h with Alexa Fluor 488- and/or 568-conju-

gated secondary antibody (Invitrogen) diluted 1:1,000. Coverslips were counterstained with 1 μg/mL Hoechst 33258 in PBS and mounted with UltraLong antifade reagent (Invitrogen). Cells positive for phospho-H2AX (defined as having >10 foci per cell) were counted on a Zeiss Axioplan microscope. Confocal images were captured on a Zeiss LSM 710 scanning confocal microscope with a 100×/1.4 N.A. oil-immersion objective. Quantitation and image processing were performed with the Zeiss Zen software package and Adobe Photoshop CS3.

Nonhomologous End Joining (NHEJ) Assay. Pem1-Ad2-EGFP plasmid was digested with either HindIII or I-SceI for 12 h and gel-purified with a Qiagen gel extraction kit. Linearized pEGFP-Pem1-Ad2 (4 μg) was cotransfected with 4 μg of pCherry by electroporation using a 280 V, 10 ms pulse delivered by a square-wave electroporator. Four hours after electroporation, medium was supplemented with the broad-spectrum caspase inhibitor QVD-OPhe at 5 μM (SM Chemicals) in addition to the indicated concentration of ABT-888. After exposure for 72 h, cells were trypsinized, washed in PBS, and fixed in 2% (wt/vol) paraformaldehyde in PBS. Flow cytometry was performed on a Becton Dickinson LSR II flow cytometer (BD Biosciences). Results are reported as a ratio of double-positive cells ($EGFP^+$/$Cherry^+$) to the total number of Cherry-positive cells, to normalize for transfection efficiency.

Microhomology-Mediated End Joining (MMEJ). A previously described assay for MMEJ activity was used (13–15). Briefly, 2 μg of EcoRV-linearized and AfeI-linearized (NEB) pDVG94 (kindly provided by Z. Lou, Mayo Clinic) was electroporated into cells. At 4 h after transfection, PEO1 and PEO4 cells were exposed to varying concentrations of ABT-888 for 72 h. After exposure, plasmid DNA was recovered by using a Hirt extraction method, phenol-chloroform–extracted twice, exposed to 25 U of proteinase K (Roche) for 1 h at 37 °C, and ethanol–precipitated. Purified DNA was PCR-amplified with primers FM30 and DAR5 (14). DNA was then digested with BstXI (NEB) for 2 h at 37 °C. Restriction fragments were separated on a 4% sieving MetaPhor agarose gel (Lonza), stained with ethidium bromide, and visualized with a UV light source. As a positive control, M059J cells lacking DNA-PKcs were used. It has been previously documented that these cells participate in MMEJ, whereas their paired DNA-PK reconstituted cells do not (15).

HPRT Mutagenesis. CAPAN1 cells were cultured in RPMI 1640 medium containing 15% FCS (medium E) in the presence of ABT-888 and/or 250 nM AZ12594248 for 72 h, washed, and allowed to recover in drug-free medium for 5 d. Each sample group was trypsinized, replated at 10^6 cells per 100-mm dish in medium E supplemented with 15 μM 6-TG, cultured until colonies were visible (14–21 d), and analyzed manually for colony formation. At the same time as 6-TG selection, 1,000 cells from each sample were plated on triplicate 60-mm dishes in drug-free medium E and allowed to grow into colonies to determine plating efficiency. Mutagenesis frequencies were calculated by dividing the number of colonies on 6-TG–treated plates by the total number of possible colonies (10^6 cells × plating efficiency).

1. Sakai W, et al. (2009) Functional restoration of BRCA2 protein by secondary BRCA2 mutations in BRCA2-mutated ovarian carcinoma. *Cancer Res* 69:6381–6386.
2. Scully R, et al. (1999) Genetic analysis of BRCA1 function in a defined tumor cell line. *Mol Cell* 4:1093–1099.
3. Zhang X, et al. (2009) Artemis is a negative regulator of p53 in response to oxidative stress. *Oncogene* 28:2196–2204.
4. Nimura Y, et al. (2007) Silencing Ku80 using small interfering RNA enhanced radiation sensitivity in vitro and in vivo. *Int J Oncol* 30:1477–1484.
5. Waninger S, et al. (2004) Identification of cellular cofactors for human immunodeficiency virus replication via a ribozyme-based genomics approach. *J Virol* 78:12829–12837.
6. Kameoka M, et al. (2004) RNA interference directed against Poly(ADP-Ribose) polymerase 1 efficiently suppresses human immunodeficiency virus type 1 replication in human cells. *J Virol* 78:8931–8934.
7. Brem R, Hall J (2005) XRCC1 is required for DNA single-strand break repair in human cells. *Nucleic Acids Res* 33:2512–2520.
8. Luo H, et al. (2004) A new XRCC1-containing complex and its role in cellular survival of methyl methanesulfonate treatment. *Mol Cell Biol* 24:8356–8365.
9. Kaufmann SH, et al. (1997) Altered formation of topotecan-stabilized topoisomerase I-DNA adducts in human leukemia cells. *Blood* 89:2098–2104.
10. Smith PK, et al. (1985) Measurement of protein using bicinchoninic acid. *Anal Biochem* 150:76–85.
11. Kaufmann SH (2001) Reutilization of immunoblots after chemiluminescent detection. *Anal Biochem* 296:283–286.
12. Segovis CM, et al. (2009) PI3K links NKG2D signaling to a CrkL pathway involved in natural killer cell adhesion, polarity, and granule secretion. *J Immunol* 182:6933–6942.
13. Fattah F, et al. (2010) Ku regulates the non-homologous end joining pathway choice of DNA double-strand break repair in human somatic cells. *PLoS Genet* 6:e1000855.
14. Verkaik NS, et al. (2002) Different types of V(D)J recombination and end-joining defects in DNA double-strand break repair mutant mammalian cells. *Eur J Immunol* 32:701–709.
15. Lou Z, et al. (2004) MDC1 regulates DNA-PK autophosphorylation in response to DNA damage. *J Biol Chem* 279:46359–46362.

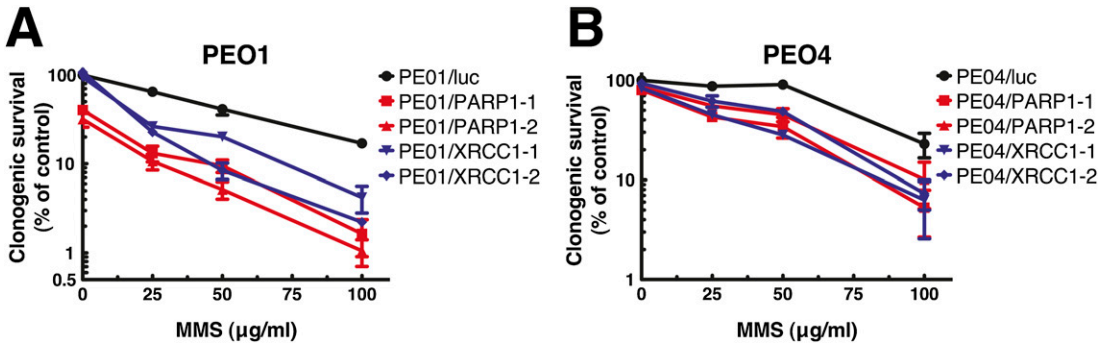

Fig. S1. siRNA knockdown of PARP1 or XRCC1 induces a base excision repair defect. MMS clonogenic survival curves of PEO1 cells (*A*) or PEO4 cells (*B*) after siRNA-directed knockdown of luciferase (control), PARP1, or XRCC1. After knockdown, cells were plated, allowed to adhere, and treated with the indicated concentration of MMS for 1 h. The plates were then washed and allowed to form colonies in drug-free medium. Results are reported as mean ± SEM of triplicate plates. Results are representative of three independent experiments.

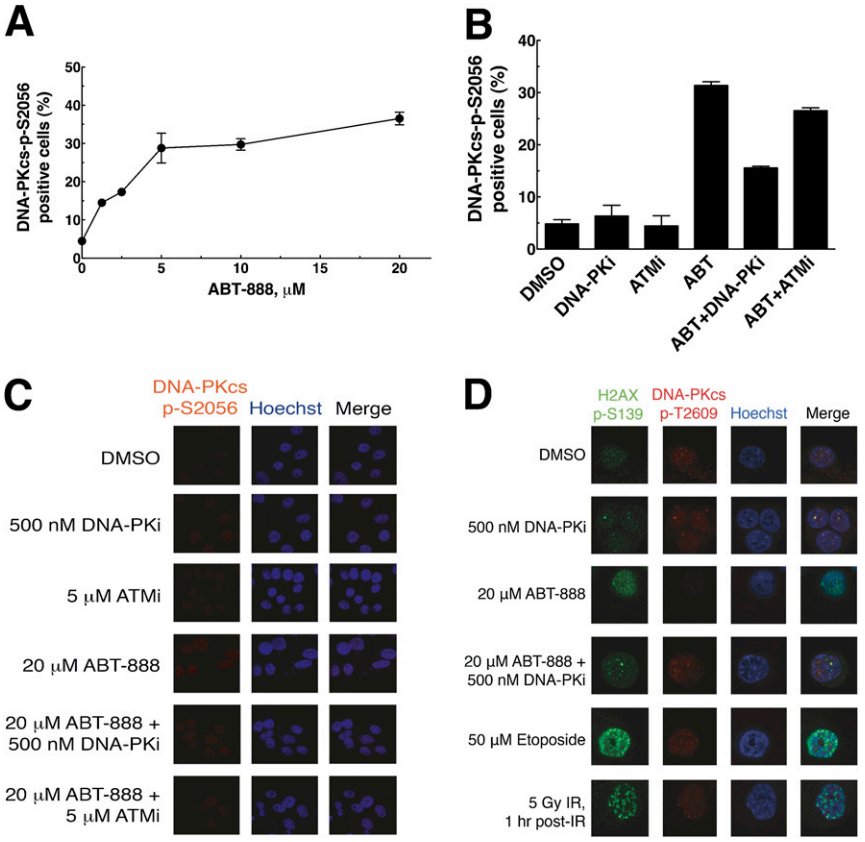

Fig. S2. PARP inhibition induces phosphorylation of DNA-PKcs selectively in PEO1 cells. (*A*) Quantitation of PEO1 cells positive for phospho-Ser^{2056} DNA-PKcs foci after 72 h exposure to increasing concentrations of ABT-888. (*B*) Quantitation of PEO1 cells positive for phospho-Ser^{2056} DNA-PKcs foci after 72 h exposure to diluent (0.2% DMSO), 500 nM DNA-PK inhibitor (DNA-PKi), 5 μM ATM inhibitor (ATMi) alone (columns 1–3) or with 20 μM ABT-888 (columns 4–6). (*C*) Representative confocal images of PEO1 cells from *B*. (*D*) Confocal images of PEO4 cells treated as indicated in Fig. 2*D*. Phospho-H2AX is shown in green, phospho-Thr^{2609} DNA-PKcs is shown in red, and Hoechst 33258 is shown in blue. Results in *A* and *B* are presented as means ± SEM of three independent experiments.

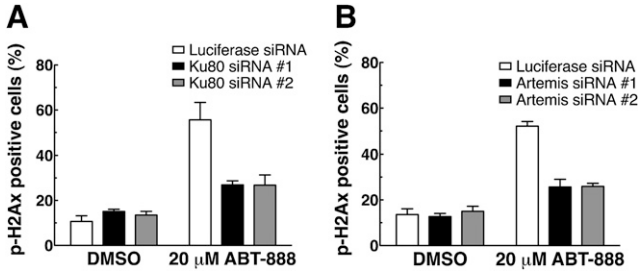

Fig. S3. siRNA-mediated knockdown of nonhomologous end joining (NHEJ) components reduces ABT-888–induced formation of phospho-H2AX foci. PEO1 cells, after siRNA-mediated knockdown of Ku80 (*A*) or Artemis (*B*), were exposed to either diluent (0.1% DMSO) or 20 μM ABT-888 for 72 h, fixed, and stained for phospho-H2AX foci. Positive nuclei were defined as having >10 foci. Results are presented as means ± SEM of three independent experiments.

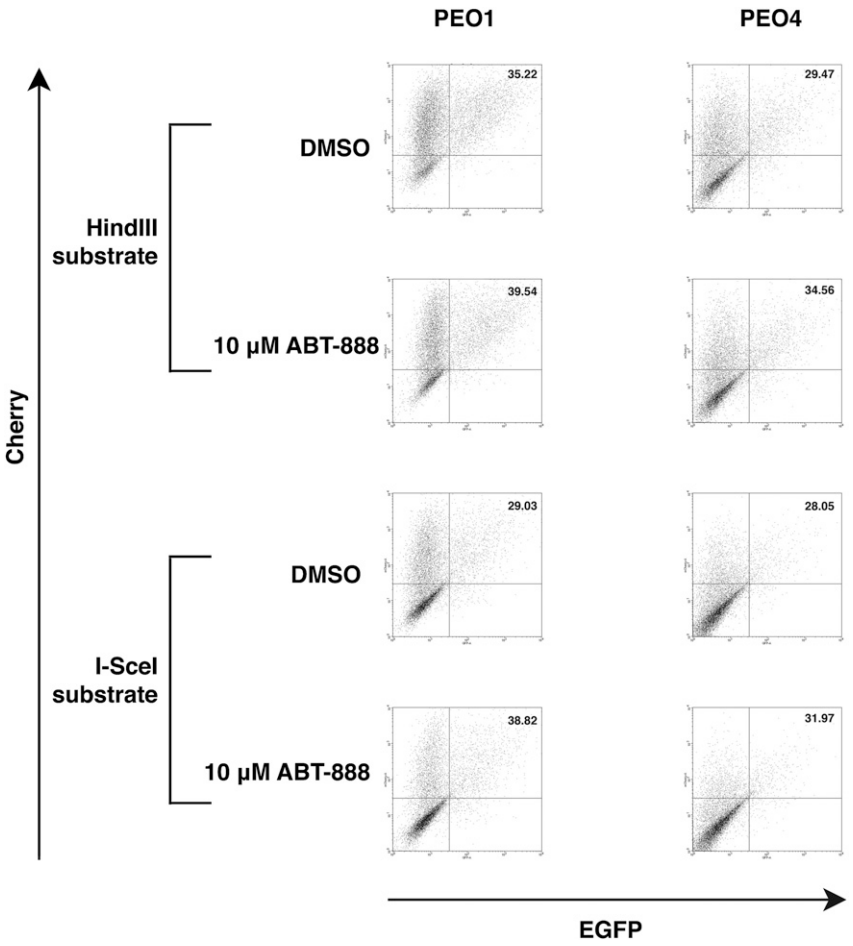

Fig. S4. ABT-888 induces NHEJ as measured by an in vivo substrate assay. Representative dot plots of PEO1 (*Left*) or PEO4 (*Right*) cells that were assayed for end joining by flow microfluorimetry. Cells were transfected with HindIII-linearized Pem1-Ad2-EGFP (upper two rows) or I-SceI–linearized Pem1-Ad2-EGFP (lower two rows) and exposed to either DMSO or 10 μM ABT-888 for 72 h. The number of double-positive ($EGFP^+/Cherry^+$) cells relative to total Cherry-positive cells was calculated to determine end joining. The percentage of transfected cells expressing repaired plasmid is shown in the upper right-hand corner of each plot.

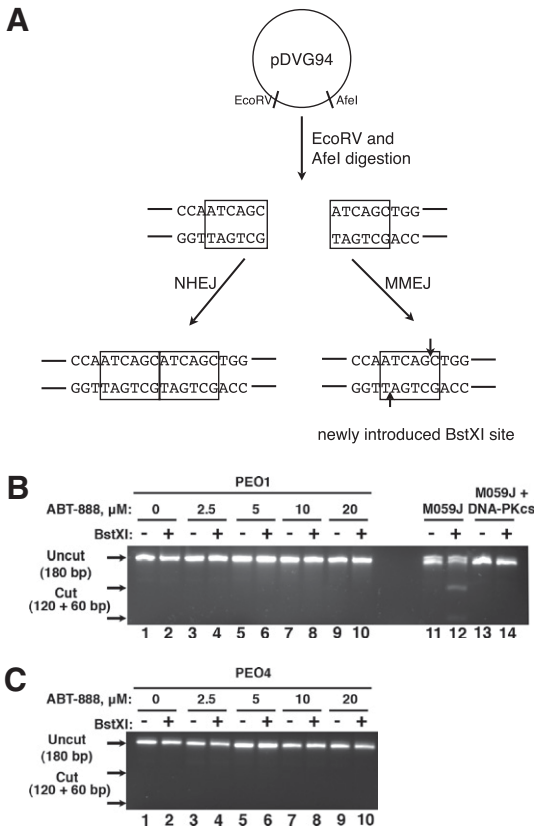

Fig. S5. PARP inhibition fails to induce MMEJ. (*A*) Schematic of the reporter substrate used to assay for MMEJ activity. Cleavage of pDVG94 with EcoRV and AfeI creates a blunt-ended linearized substrate, with identical 6-bp ends. Direct joining by NHEJ will result in maintenance of both repeats, but MMEJ will excise one repeat, introducing a new BstXI site. PCR across recircularized substrate produces a product of 180 bp, which can be cut into 120- and 60-bp fragments if the BstXI site is created. This schematic is adapted from Verkaik et al. (1). (*B* and *C*) Agarose gel from a representative MMEJ assay. PEO1 (*B*, lanes 1–10) and PEO4 (*C*) cells were treated with increasing concentrations of ABT-888 after transfection with linearized pDVG94. The size of the initial PCR product (180 bp) as well as BstXI-cleaved products (120 bp and 60 bp) are indicated. As a positive and negative control, a cell line previous documented to undergo MMEJ (2), M059J (*B*, lanes 11 and 12) and a MMEJ-negative line, M059J+DNA-PKcs (*B*, lanes 13 and 14), were used. Images were captured from one gel and cut to create two panels.

1. Verkaik NS, et al. (2002) Different types of V(D)J recombination and end-joining defects in DNA double-strand break repair mutant mammalian cells. *Eur J Immunol* 32:701–709.
2. Lou Z, et al. (2004) MDC1 regulates DNA-PK autophosphorylation in response to DNA damage. *J Biol Chem* 279:46359–46362.

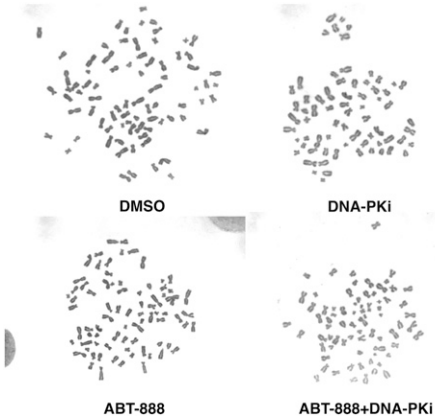

Fig. S6. PARP inhibition fails to induce chromosomal instability in BRCA2-positive PEO4 cells. Representative metaphase spreads from PEO4 cells treated with 0.2% DMSO, 500 nM DNA-PK inhibitor (DNA-PKi), 2.5 μM ABT-888, or both DNA-PK inhibitor and ABT-888.

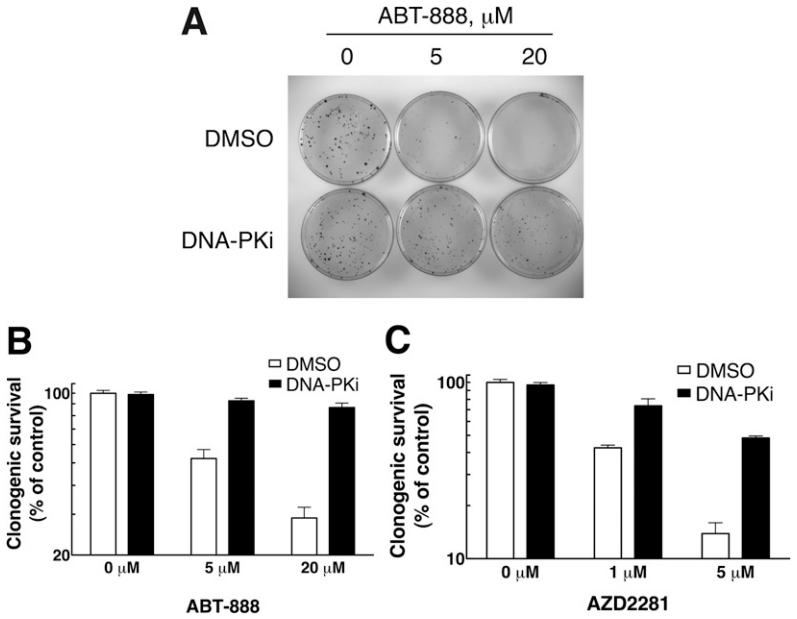

Fig. S7. DNA-PK inhibition diminishes the lethality of multiple PARP inhibitors in PEO1 cells. (*A*) Representative clonogenic plates after PEO1 cells were treated with ABT-888 (0, 5, or 20 μM) with or without 500 nM DNA-PK inhibitor (DNA-PKi). (*B* and *C*) Bar graphs comparing clonogenic survival of PEO1 cells exposed to two PARP inhibitors with or without 500 nM DNA-PK inhibitor. The PARP inhibitors used for these assays are ABT-888 (*B*) and AZD2281/olaparib (*C*). Results are reported as mean ± SEM of triplicate plates.

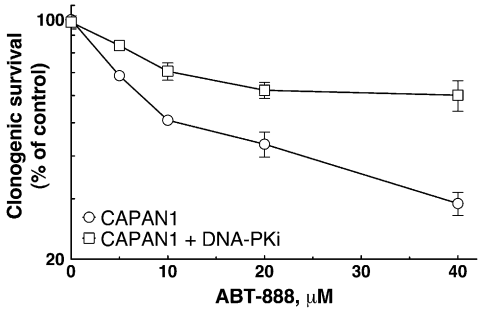

Fig. S8. PARP inhibitor sensitivity of BRCA2-mutant CAPAN1 cells is diminished by DNA-PK inhibition (DNA-PKi). Clonogenic survival curve of CAPAN-1 cells treated with increasing concentrations of ABT-888 with or without 250 nM DNA-PK inhibitor.

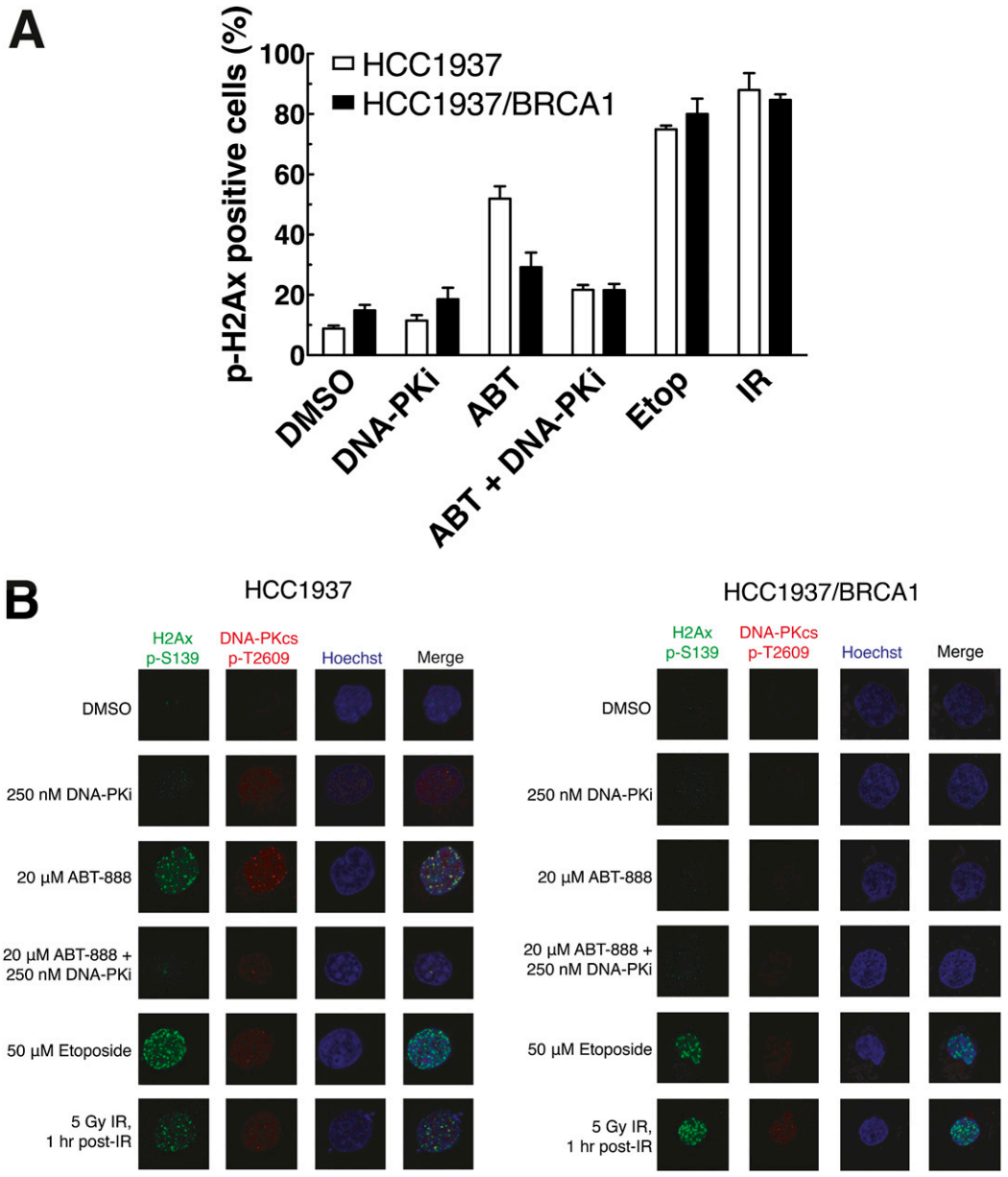

Fig. S9. Upon PARP inhibition, HCC1937 cells form phospho-H2AX foci that colocalize to regions of activated DNA-PK. (*A*) Quantitation of cells positive for phospho-H2AX foci in HCC1937 and HCC1937/BRCA1 cells, after treatment with 0.2% DMSO, 250 nM DNA-PK inhibitor (DNA-PKi), 20 μM ABT-888 (ABT), ABT-888 and DNA-PK inhibitor, 50 μM etoposide (Etop), or 5 Gy of ionizing radiation (IR). Cells were exposed to ABT-888 and/or DNA-PK inhibitor for 72 h, etoposide for 1 h, or allowed to recover 1 h post-IR. Results are reported as mean ± SEM of three independent experiments. (*B*) Confocal microscopy after staining with antibodies to phospho-H2AX (Ser^{139}) and phospho-DNA PKcs (Thr^{2609}) as in Fig. 2*D*. HCC1937 cells are shown on the *Left*, and reconstituted HCC1937/BRCA1 cells are shown on the *Right*.